ADSORPTION AND SURFACE DISSOCIATION OF HNCO ON Pt(110) SURFACES: LEED, AES, ELS AND TDS STUDIES

F. SOLYMOSI and J. KISS

Reaction Kinetics Research Group, The University, P.O. Box 105, H-6701 Szeged, Hungary

The interaction of HNCO with Pt(110) surface has been investigated by different techniques at low and high-temperatures. The adsorption of HNCO on Pt(110) caused no reordering of the surface Pt atoms from the (1 × 2) to the (1 × 1) structure. At saturation, an ordered (2 × 2) structure was formed, HNCO was detected in the desorbing gases only after its low temperature (110 K) adsorption; it desorbed in two stages, with peak maxima at 150 and 270 K. In addition, the formation of H_2 ($T_{max} \sim 290$ K) and NH_3 ($T_{max} \sim 293$ and 390 K) was also observed. When the temperature was raised to above 400 K, N_2 and CO evolution was noticed, but neither NCO nor (NCO)$_2$ species were found in the desorbing gases. The adsorption of HNCO at 110 K produced a very intense loss at 10.4 eV and a less intense one at 13.5 eV in the electron energy loss spectra. From the behaviour of these losses at higher temperature it was inferred that the dissociation of adsorbed NCO species to adsorbed N and CO begins to an appreciable extent above 230 K, and that the dissociation is complete at 310–330 K. It is proposed that NCO is located in the "trough sites" of the corrugated surface of (1 × 2) structure and that it is multiply bonded to the Pt atoms.

1. Introduction

Recent infrared spectroscopic studies revealed that in the high-temperature reaction between NO and CO on supported metals an isocyanate complex is formed [1–6]. Different opinions have been expressed regarding the role of this complex in the NO + CO reaction. While it was originally thought that this species is a real surface intermediate of this reaction [1,2], recent data suggest that it is possibly responsible for the desactivation of the catalyst [7,8]. On the other hand, there is strong evidence indicating, that although NCO is formed on the metal, it migrates in a fast process onto the support, or to the metal–support interface, and it is the support that primarily determines the reactivity of the NCO species [9,11].

In order to acquire a clearer picture concerning the reactivity of the NCO species on metals, it is desirable to investigate its behaviour on clean surfaces under ultra-high vacuum conditions. To date the surface behaviour of the NCO species has been examined by modern surface techniques only on the Cu(111) face [12]. As the NCO surface complex can not be produced by the NO + CO reaction at low pres-

sure, isocyanide acid (HNCO) was applied as adsorbing species. On a clean Cu(111) surface no adsorption of HNCO was detected at 300 K. However, preadsorbed oxygen exerted a dramatic influence, and caused the dissociative adsorption of HNCO with concomitant release of water. Decomposition in the adsorbed phase started above 400 K, with the evolution of CO_2. At higher temperatures, the desorptions of N_2 (>700 K) and C_2N_2 (>800 K) were observed. Since neither CO nor CO_2 is bonded to Cu surfaces under ultrahigh vacuum at 300 K, it was concluded that NCO exists as such on a Cu(111) surface, and the desorption temperature of CO_2 very likely corresponds to the *reaction* temperature between the adsorbed species NCO and O. This conclusion seems to be supported by the results of electron energy loss spectroscopic measurements; new loss features appeared at 10.4 and 13.5 eV, which were not observed after exposure of the Cu surface at 300 K to any of the desorption or decomposition products of NCO.

In the present work a report is given of the surface chemistry of NCO on the Pt(110) surface, studied by LEED, Auger, electron energy loss and thermal desorption spectroscopy, again with HNCO as adsorbing species. The majority of the measurements were carried out after room-temperature adsorption of HNCO, but some low-temperature experiments were also performed.

2. Experimental

Experiments have been performed in a stainless steel UHV chamber equipped with several gas inlets, a single-pass cylindrical mirror analyzer for Auger electron spectroscopy (AES), a three-grid retarding field analyzer for low-energy electron diffraction (LEED) to determine surface structure, and a quadrupole mass analyzer to monitor gas-phase composition. The vacuum system was evacuated with ion pumps and a titanium getter. A base pressure of $(1-3) \times 10^{-10}$ Torr was reached.

Auger spectra were taken with 4 V peak-to-peak modulation, $1-10$ μA of incident current, 2.5 kV of incident energy, and a sweep rate of 3 V/s.

For electron energy loss spectra the gun of CMA was used as a primary electron source with energies between $20-125$ eV and a beam current of $0.2-1.0$ μA. The backscattered electrons were analyzed with CMA. A modulation voltage of 0.1 eV was found to be the optimum for the used system. The velocity of taking a spectrum was 0.4 eV/s. The exact position of the peak maxima of energy losses were determined by a Keithley electrometer. Electron energy loss spectra were taken in $dN(E)/dE$ form.

The Pt crystal was cut from single crystal rod of ultrahigh purity platinum (5N) obtained from Materials Research Corporation. The sample was mechanically polished and etched briefly with aqua regia before placing in the vacuum chamber. The platinum slice was spot-welded between two tungsten wires which themselves were fixed to two Mo roads mounted on crystal manipulator. The sample was heated resistively, the temperature was measured with a chromel−alumel thermo-

couple spot-welded to the edge of the crystal. For low temperature measurements the sample was cooled through a 0.5 mm platinum wire attached to a liquid-nitrogen-cooled stainless-steel tube.

The sample was cleaned by heating at 1300 K for several hours followed by argon ion bombardment to remove phosphorus, oxygen, calcium and the main part of carbon as major contaminants. The remaining carbon was removed by brief reaction with oxygen at 900 K. Finally the sample was annealed at 1300 K. This cleaning procedure was repeated until the Auger spectrum showed Pt transitions only. The clean annealed surface was characterized by a (1 × 2) LEED pattern.

HNCO was prepared by the reaction of saturated aqueous KNCO solution with 95% H_3PO_4 at 300 K [13]. The product was purified several times by bulb-to-bulb distillation under HV and UHV conditions. HNCO was introduced into the chamber from an auxiliary vacuum system pumped by a small (8 l/s) ion pump through a stainless steel tube with a diameter of 0.8 mm. The crystal face was positioned about 0.5 cm in front of the effusion hole. The pressure was calculated from the molecular flow conditions and the dimensions of the hole [14].

3. Results

3.1. Adsorption at 300 K

3.1.1. Auger studies

The Auger spectrum of a cleaned Pt(110) surface is shown in fig. 1. Exposure of the clean (1 × 2) surface to HNCO at 300 K resulted in the appearance of the C, N
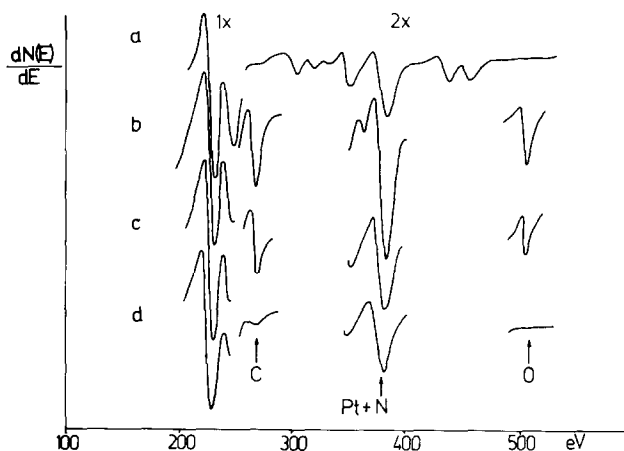

Fig. 1. Auger spectra of the Pt(110) surface: (a) clean surface; (b) after exposure to 60 L HNCO at 300 K; (c) after heating the sample exposed to 60 L HNCO to 478 K; (d) after heating the sample exposed to 60 L HNCO to 600 K.
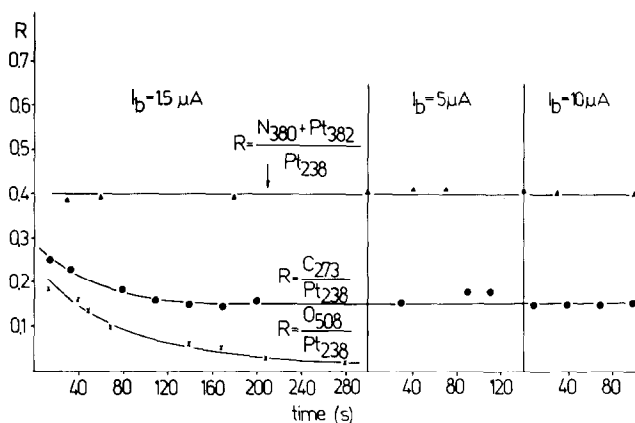
Fig. 2. The effect of the beam current and beam exposition on the relative intensities of N, C and O Auger signals. The surface was exposed to 60 L HNCO at 300 K.

and O KLL signals at 273, 380 and 508 eV (fig. 1). Before conducting more detailed measurements, we investigated the effect of an electron beam. The results obtained are shown in fig. 2.

As the signals of N (380 eV) and Pt (382 eV) cannot be separated, the values of $(N_{380} + Pt_{382})/Pt_{238}$ were calculated. The value of this ratio for the clean Pt surface is 0.194. A decrease in the relative intensity of the O signal was observed when the adsorbed layer was exposed even to a low value (1.5 μA) of the electron beam current. Less effect was detected in the carbon signal, and practically no change occurred in the N signal, even at high beam current. In order to reduce the effect of the beam, the Auger spectra were generally recorded at low beam current. In addition, the important signals were always measured first. Taking into account the Pt signal at 238 eV on the clean surface, as well as the relative sensitivity of Auger electron spectroscopy as regards carbon and nitrogen ($\sim$1.5), we obtain a value of approximately 1 for the carbon/nitrogen ratio, in agreement with that expected from isocyanate.

In fig. 3 the intensities of the C and N signals are plotted as functions of the HNCO exposure. It can be seen that the relative intensities of the N and C signals reach a saturation value above 20 L. When the relative intensity of the C signal is plotted against that of the N signal, a straight line is obtained.

Calculation of the surface coverage was attempted from the measured relative intensity of the N signal. The measurements of Gland [15] showed that a relative intensity of the N signal $(N_{380} + Pt_{382})/Pt_{238}$ of 0.54 in the Auger spectra corresponds to $(4 \pm 1) \times 10^{14}$ N atoms/cm^2. As the relative intensity of the N signal at saturation was 0.48 $\pm$ 0.02 in the present case, we obtained a value of $(3.1 \pm 1) \times 10^{14}$ molecules/cm^2 for the saturation coverage. (The slight difference between the
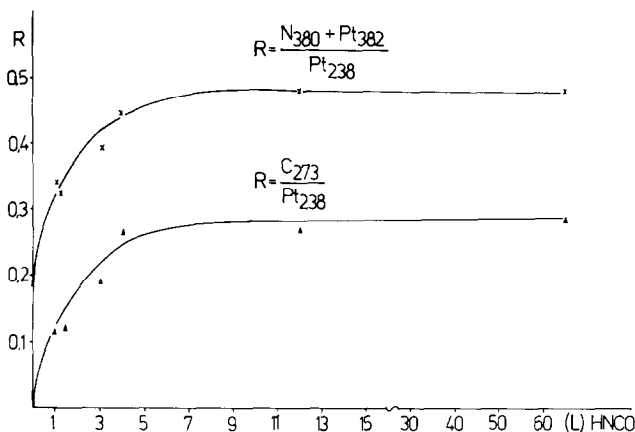
Fig. 3. The dependence of the relative N and C signals on the HNCO exposure (E_p = 2.5 kV, I_b = 1.5 μA).

Auger spectra of our clean sample and that of Gland was taken into account in the calculation.) A similar value was obtained by calculations based on the relation between the amount of adsorbed oxygen and the relative oxygen signal in the Auger spectra, determined independently by two research groups [16,17]. Considering the amount of desorbed nitrogen after saturation, and the sensitivity of our mass-spectrometer towards nitrogen and oxygen, we obtained 3.7×10^{14} molecules/cm^2.

The sticking coefficients have been graphically estimated from plots of the relative N Auger signal as a function of the total exposure; we obtained a value of 0.34.

3.1.2. LEED studies

The clean annealed Pt(110) surface showed a (1 × 2) LEED pattern (fig. 4). When as little as 0.45 L HNCO was adsorbed at 300 K, a slight change was observed in the LEED pattern. Exposure of the surface to at least 4.8 L HNCO produced a (2 × 2) LEED pattern with a diffuse background (fig. 4). This diffuse scattering indicates a certain structural disorder due to the adsorbate.

No further structural change was experienced with further increase of the HNCO exposure. When the sample was heated to 485 K, the majority of the N was desorbed (see thermal desorption measurements) and then cooled to 300 K, the (1 × 2) structure appeared again.

3.1.3. Thermal desorption studies

Thermal desorption spectra were taken at a linear heating rate of 13 K s^{-1}. A small amount of NH$_3$ desorbed at the lowest temperature, its desorption maximum
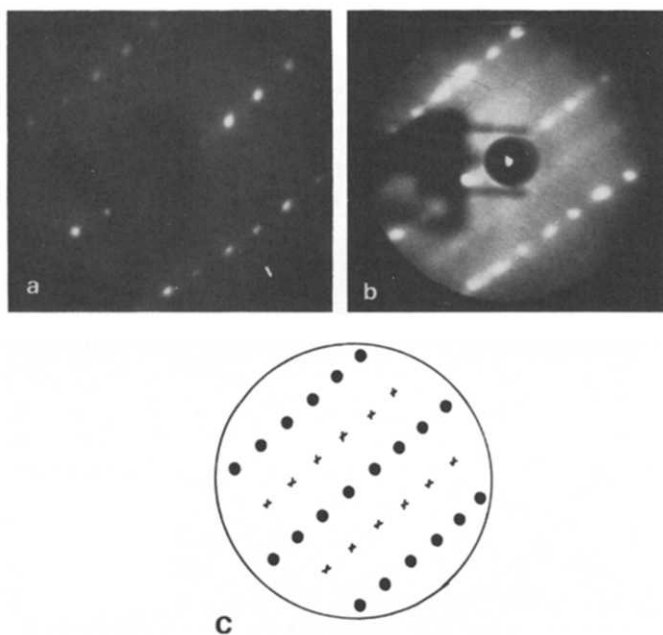
Fig. 4. (a) LEED pattern from clean Pt(110) surface; (b) LEED pattern at 81 V from HNCO saturated surface; (c) A schematic representation of the LEED pattern (b).
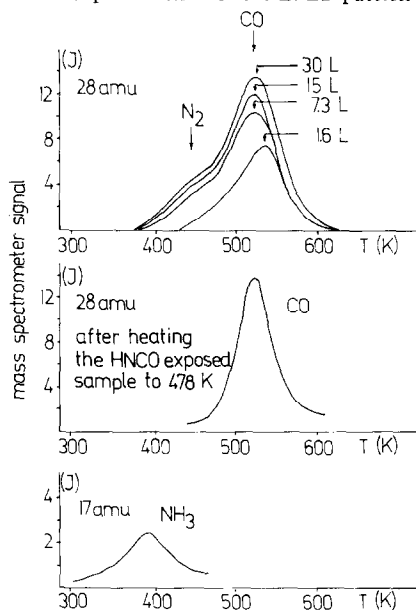

Fig. 5. Thermal desorption spectra following HNCO adsorption at 300 K on Pt(110) surface. The curves are uncorrected for detection sensitivities.

was at 390 K (fig. 5). Traces of H_2 were also identified at 300–400 K. It should be mentioned that during the adsorption of HNCO we detected the formation of H_2; its amount was greater than that arising from the fragmentation of HNCO. Interestingly, there was no detectable desorption of HNCO, NCO radical or $(NCO)_2$, and in contrast with the situation in the case of the Cu(111) surface we could not demonstrate the formation of C_2N_2. The major signal was at 28 amu (CO and N_2). The peak is not symmetrical: a shoulder can easily be identified on the lower-temperature side of the peak (fig. 5). CO and N_2 can be expected as the main products, and it thus seemed very likely that the 28 amu peak is due to desorbed CO and N_2. As labelled HNCO was not available, a differentiation between N_2 and CO was attempted by measuring the signal at 14 amu (N^+). From these measurements it can be concluded that the majority of the N_2 is desorbed at a lower temperature, and the CO at higher temperature. When the thermal desorption was interrupted at 478 K, Auger analysis of the sample cooled to 300 K showed a much weaker signal due to N, the intensity of the C signal, however, remaining practically the same as before the thermal desorption (fig. 1, curve c). On continuation of the thermal desorption, we now obtained an almost symmetrical desorption spectrum (fig. 5). No C and O signals were identified afterwards in the Auger spectra (fig. 1, curve d).

The peak temperature of the desorption of N_2 ($T_{max} \sim 458$ K) varied only slightly with the increase of the coverage. Using the equation derived by Redhead, and with a pre-exponential factor of 10^{13} s^{-1}, we obtained 115 kJ mol^{-1} for the activation energy of the desorption of N_2. The desorption temperature of CO (528 K) was almost independent of the coverage; the activation energy was 130 kJ mol^{-1}. The results of thermal desorption measurements are given in table 1.

3.1.4. Electron energy loss measurements

Attempts were made to follow the adsorption of HNCO by electron energy loss

Table 1
Summary of the results of TDS measurements on Pt(110) surface

State [a]	T_{max} (K)	E [b] (kJ/mol)	Ref.
HNCO/HNCO [d]	270	66.2	This work
NH$_3$/HNCO [d]	293	72.1	This work
NH$_3$/HNCO	390	96.8	This work
N$_2$/HNCO	458	115.0	This work
CO/HNCO	528	130.0	This work
N$_2$/N [c]	450	104.5	[29]
CO/CO	508	129	[24]

[a] The notation of A/B refers to desorption peak for gas A following adsorption of gas B.
[b] Calculated from the observed values of T_{max} with a pre-exponential factor of 10^{13} s^{-1}.
[c] Calculated on base of heating rate variation method.
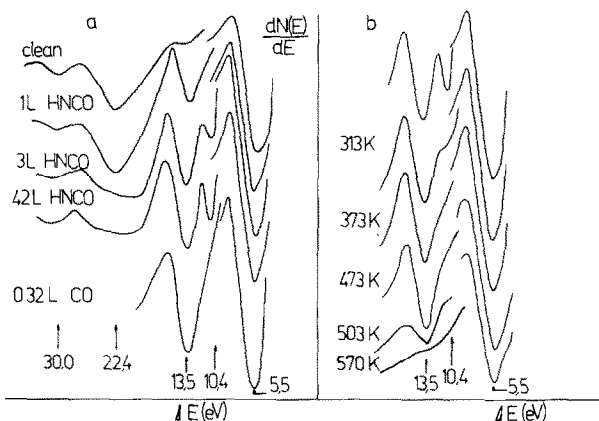[d] Adsorption at 110 K.

Fig. 6. (a) Electron energy loss spectra of Pt(110) as a function of HNCO exposure at 300 K; for comparison, the spectra of clean Pt(110) surface and that exposed to 0.32 L CO are also shown (E_p = 70 eV, I_b = 0.2 μA). (b) Electron energy loss spectra taken after heating the sample to different temperatures. The surface was exposed to 60 L HNCO at 300 K before heating.

spectroscopy. The differentiated loss spectrum of clean Pt(110) for an electron beam at normal incidence and with an energy of 70 eV is shown in fig. 6. The energy loss is measured as the difference between the negative excursion energy of the primary beam and that of the loss peak. The main energy losses of Pt(110) in table 2 show a good agreement with the loss features of other Pt surfaces [18,19].

As a consequence of HNCO adsorption, a slight decrease of the Pt loss was detected at 22.4 eV. This may support the assignment of Seignac and Robin [20] that this loss is probably due to surface plasmons. An enhancement of the loss at 5.1–5.5 eV can also be observed. The intensities of elastically reflected electrons increased considerably; a possible reason for this is that C, N and O may have elastic backscattering cross-sections much greater than those of the high atomic number atoms of the substrate [21,22]. Even at an HNCO exposure of 1 L, an intense new loss appeared at 13.5 eV. As the HNCO exposure increased, the 13.5 eV loss intensified only slightly, but a loss feature at 10.4 eV became well discernible. In order to minimize the effect of the beam, a similar approach was used as in the case of the Auger measurement, i.e. the new losses produced by the adsorption of HNCO were always taken first. The loss at 10.4 eV disappeared when the sample was heated above 313 K, while that at 13.5 eV was eliminated above 573 K (fig. 6). (The heating rate was 13 K s^{-1}, and the sample was kept at the selected temperature for 30 s.)

For comparison we also show the loss spectrum of adsorbed CO. In this case an

Table 2
Characteristic energy losses of Pt surface covered with different adsorbates

Pt sample	E_p (eV)	Clean metal losses					New losses after adsorption of				Adsorption temperature (K)	Ref.
							HNCO		CO			
Pt (110)	70	5.1	5.5	(12.5)	22.4	30	10.4 (s)	13.5 (w)			110	This work
Pt (110)	70	5.1	5.5	(12.5)	22.4	30	10.4 (w)	13.5 (s)	13.5	(s)	300	This work
Pt (100)	71–205	6.5	(12)	(15)	24	33			6	13.5	300	[18,19]

w = weak loss, s = strong loss, numbers in brackets correspond to very weak losses.

intense loss feature appeared at 13.5 eV and an enhancement of the loss at 5.1–5.5 eV was also observed (fig. 6).

3.2. Adsorption at 110 K

As we could not identify HNCO in the desorbing gases after adsorption at 300 K, we performed some low-temperature (110 K) adsorption measurements. In this case the adsorption of HNCO was greatly increased, as indicated by Auger and flash desorption measurements. The desorption of HNCO (43 amu) was observed even at the beginning of heating (the heating rate in this case was ~ 7 K s^{-1}); the desorption occurred in two stages, with peak maxima at 150 and 270 K (fig. 7). In addition we observed the desorption of H_2 ($T_{max} = 290$ K) and the formation of NH_3 at 293 and ~ 390 K (fig. 7). No other gases (N_2, CO, CO_2, H_2O) desorbed in this low temperature range, however. On interrupting the heating at 300 K, we could detect the Auger signals due to N, C and O. On the basis of their relative intensities, the coverage corresponds to that achieved by exposing the sample to 60 L HNCO at 300 K. The desorption of N_2 and CO occurred at almost the same temperatures as after adsorption at 300 K.

Electron energy loss measurements at low temperature were complicated by the fact that the adsorption of CO from the background also caused a weak loss at
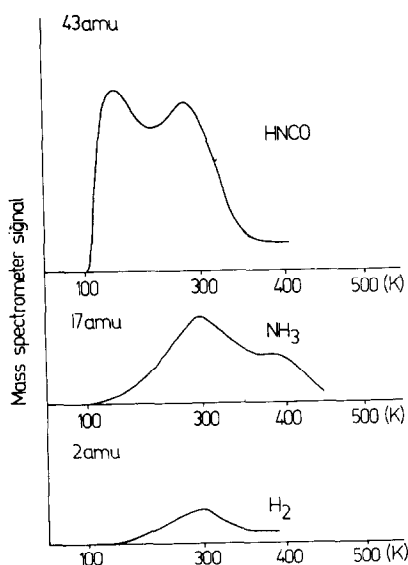

Fig. 7. Thermal desorption spectra following HNCO adsorption at 110 K on Pt(110) surface. The HNCO exposure was 60 L. The curves are uncorrected for detection sensitivities.
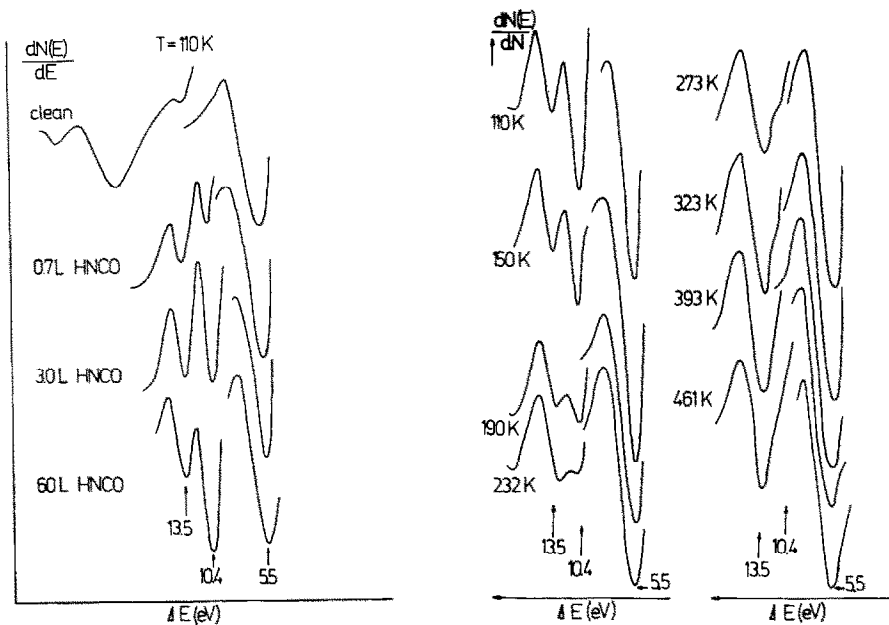
Fig. 8. Electron energy loss spectra of Pt(110) as a function of HNCO exposure at 110 K (E_p = 70 eV, I_b = 0.2 μA).

Fig. 9. Electron energy loss spectra taken after heating the sample to different temperatures. The surface was exposed to 60 L HNCO at 110 K before heating.

13.5 eV, and we could not eliminate this effect completely. The adsorption of HNCO at 110 K again caused an attenuation of the loss at 22.4 eV, and produced a very intense loss at 10.4 eV and an enhancement of the loss at 13.5 eV (fig. 8). When the sample was heated to higher temperatures, the loss at 10.4 eV was gradually eliminated at 110–330 K. The intensity of the loss at 13.5 eV decreased somewhat from 110 K to 190 K. Afterwards it increased significantly up to about 323 K. It began to decrease above 461 K, and it disappeared at 573 K, similarly as after adsorption at room temperature (fig. 9).

4. Discussion

4.1. General characteristics of adsorption and dissociation of HNCO on Pt

The Pt(110) face displays the interesting behaviour that it has a stable (1 × 2) and a metastable (1 × 1) LEED pattern. As a result of thermal treatment and an

electron beam, the (1 × 1) is easily transformed into the (1 × 2) structure. The adsorption of numerous gases (NO, CO, C_2N_2, C_2O_3 and HCN), however, changes the surface periodicity from (1 × 2) to (1 × 1) [23–28]. We recently found that higher coverages of adsorbed N atoms also cause the (1 × 2) → (1 × 1) transformation [29].

In contrast to the effect of many gases, the adsorption of HNCO on Pt(110) caused no reordering of the surface Pt atoms from the (1 × 2) to the (1 × 1) structure. At saturation we observed a (2 × 2) surface structure, which means that only every second a Pt atom is covered by the adsorbate. Taking into account the area of the unit cell (21.7 $Å^2$), we find that at saturation 2.3 × 10^{14} HNCO molecules are adsorbed on 1 cm^2. This value is in agreement with those calculated on the basis of the measured relative intensity of the N signal in the Auger spectrum (see section 3.1.1).

In contrast to the Cu surface, the adsorption of HNCO on the Pt(110) face does not require the presence of preadsorbed oxygen, and the surface coverage at saturation exceeds that obtained on an oxygen-dosed Cu(111) surface by a factor of 3. The sticking coefficient in the present case was 0.34, which is higher than that on Cu(0.1).

HNCO was detected in the desorbing gases only after its low-temperature (~110 K) adsorption; it desorbed in two stages, with peak maxima at 150 and 270 K. In addition, we also observed the formation of H_2 (T_{max} ~ 290 K) and NH_3 (T_{max} ~ 293 and 390 K). The formation of H_2 suggests that some of the adsorbed HNCO is dissociated on the surface:

$$HNCO_{(a)} \rightleftharpoons H_{(a)} + NCO_{(a)}, \tag{1}$$

and, as the temperature is raised, reactions commence in the adsorbed phase. The adsorbed H atoms may recombine and desorb:

$$H_{(a)} + H_{(a)} \rightleftharpoons H_{2(g)}, \tag{2}$$

or react with adsorbed NCO species to yield the HNCO molecule:

$$H_{(a)} + NCO_{(a)} \rightleftharpoons HNCO_{(a)} \rightleftharpoons HNCO_{(g)}, \tag{3}$$
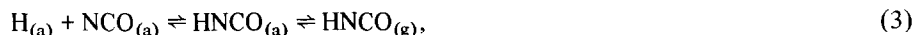
or to produce NH_3. The low desorption temperature of hydrogen on Pt surface is in agreement with the results of previous work [30]. On the other hand, the formation ⹁f NH_3 in the surface reaction between H_2 and the isocyanate species was also observed on the supported Pt catalyst [1,3]. The desorption temperature of NH_3 agrees with that following NH_3 adsorption [15].

Accordingly, we propose that in the low-temperature stage of desorption of HNCO (T_{max} ~ 150 K) the weakly bonded HNCO desorbs:

$$HNCO_{(a)} \rightleftharpoons HNCO_{(g)}, \tag{4}$$

while in the high-temperature stage (T_{max} ~ 270 K) the desorption of HNCO formed in the recombination of adsorbed H and NCO (eq. (3)) occurs. As can be

seen in fig. 7, the two processes take place almost simultaneously.

When the temperature was further raised to above 400 K, N_2 and CO evolution was observed, but neither NCO or $(NCO)_2$ species were found in the desorbing gases.

This shows that NCO formed in the dissociation of adsorbed HNCO, or in the dissociative adsorption of HNCO, is strongly bonded to the surface Pt atoms and, instead of undergoing desorption, it decomposes on the surface to adsorbed nitrogen and carbon monoxide:

$$NCO_{(a)} \rightleftharpoons N_{(a)} + CO_{(a)}. \tag{5}$$

When the adsorption of HNCO was performed at 300 K, we observed H_2 evolution even during the adsorption. A small amount of NH_3 also desorbed, but there was no detectable desorption of HNCO.

4.2. Dissociation of surface NCO species

The question arises as to the thermal stability of the NCO species on the Pt surface. The TDS measurements indicated that nitrogen desorbed above 400 K, and CO at a slightly higher temperature (above 450 K). It would be tempting to assume that the temperature of nitrogen evolution was characteristic of the stability of the NCO species on the Pt(110) face. As there were no data in the literature concerning the interaction of N atoms with the Pt(110) surface, in a separate study we examined the adsorption and desorption of N atoms on this surface [29]. Exposure of the clean Pt(110) face to 5 L (N + N_2) produced a weak additional (2 X 2) LEED pattern with a diffuse background at the surface concentration of 2.3×10^{14} atoms/cm^2. Further exposure caused a reordering of the surface Pt atoms from the (1 X 2) to the (1 X 1) structure. The desorption began above 400 K. At low coverage (up to $\theta \sim 0.25$), the maximum temperature of the peak was shifted to a lower value with the increase of the coverage. In the range $\theta = 0.25-1$, the desorption process seemed to be of the first order. The activation, energy determined by variation of the heating rate was 104.6 kJ/mole^{-1}.

As far as the desorption characteristics of CO are concerned, they agree quite well with those determined by Bonzel and Ku [23] and Comrie and Lambert [24].

Accordingly, the characteristic data for the thermal desorption of N_2 and CO determined after adsorption of HNCO at 300 K conform satisfactorily with those obtained after separate adsorption of these gases (table 1). This agreement makes it very unlikely that the temperature of nitrogen desorption represents the decomposition temperature of the NCO species. It also shows that from the thermal desorption data it is not possible to establish the dissociation temperature of the NCO species on the Pt(110) surface.

More information can be obtained for this question from ELS measurements. Let us deal first with the origin of these losses. Adsorption of HNCO at 110 K produced a strong loss at 10.4 eV, and a less intensive one at 13.5 eV. As none of the

possible decomposition and reaction products (CO, CO_2, N_2, NH_3) gave a loss at 10–11 eV, we may safely *attribute the 10.4 eV loss to the adsorbed isocyanate, HNCO and NCO species.*

The situation is more complex as regards the origin of the 13.5 eV loss, as the adsorption of CO on the Pt(110) surface also causes a loss in the 13–14 eV region (fig. 6) in harmony with the results obtained on the Pt(100) surface [18,19]. On the basis of the following considerations, as well as the behaviour of this loss, however, we believe that the enhancement of the 13.5 eV loss observed after low-temperature adsorption is also due to the adsorbed NCO species.

This assumption is strongly supported by the results obtained on the Cu(111) surface [12]. Both the 10.4 and the 13.5 eV losses appeared in the electron energy loss spectra after the room-temperature adsorption of HNCO, but in this case the contribution of adsorbed CO to the loss feature at 13.5 eV *can be entirely excluded*, as CO does not adsorb on the Cu(111) face at 300 K. The intensity of the 10.4 eV loss was much higher han that of the 13.5 eV loss, similarly as in the present case after HNCO adsorption at 110 K.

Another observation is that, in contrast to the adsorption of CO [19], exposure of the Pt surface to HNCO at 110 K caused no enhancement of the loss at 5.1–5.5 eV. From these results we may conclude that the adsorption of HNCO produces no CO at 110 K, and thus the contribution of adsorbed CO to the loss at 13.5 eV at this temperature is not greater than that caused by CO from the background.

When the sample exposed to HNCO at 110 K was heated to higher temperatures, the intensity of the 10.4 eV loss rapidly decreased from 110 K to 190 K, very likely due to the desorption of HNCO. It slightly changed up to 230 K, and decreased further above this temperature (fig. 10). It was completely eliminated at about 330
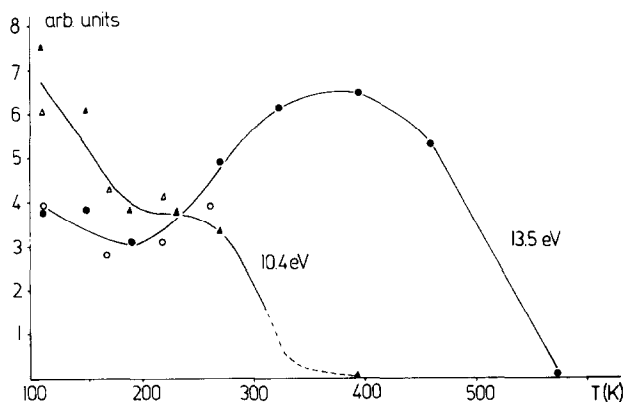

Fig. 10. The intensities of 10.4 and 13.5 eV losses after heating the sample to different temperatures. The surface was exposed to 60 L HNCO at 110 K before heating. (●), (▲) Points calculated from EEL spectra of fig. 9, (○), (△) points calculated from other EEL measurements.

K. The behaviour of the loss at 13.5 eV was more complex. After a transient decrease in its intensity up to 190 K, the intensity of this loss increased up to the temperature of the complete elimination of the 10.4 eV loss (320–330 K), and remained constant between 330 and 461 K. We assume that the decrease in the intensity of the 13.5 eV loss is also due to the desorption of HNCO (i.e. the occurrence of reactions (3) and (4), which reduces the number of surface NCO species too), while the increase of its intensity observed from 230 K can be attributed to the formation of adsorbed CO, i.e. to the surface dissociation of NCO species (reaction (5)). It appears that chemisorbed CO produces a more intense loss than that of chemisorbed NCO species in this loss region peaking at 13.5 eV, and thus its formation overcompensates the effect of desorption of HNCO and decomposition of NCO on the intensity of the 13.5 eV loss.

The behaviour of 10.4 and 13.5 eV losses may suggest that the surface dissociation of adsorbed NCO species begins to an appreciable extent above 230 K.

When the adsorption of HNCO was performed at 300 K, the predominant features in the electron loss spectrum were the intensive loss at 13.5 eV. The loss at 10.4 eV appeared only at higher HNCO exposure, and its intensity was much less than that at 13.5 eV. Accordingly, HNCO adsorbed dissociatively on the Pt(110) surface at this temperature, and the *adsorbed NCO decomposed further to adsorbed N and CO.* At higher coverage, however, some undissociated NCO remained on the surface, as indicated by the appearance of a loss at 10.4 eV. This loss was eliminated above 313 K. Note, that no desorption of HNCO was observed following the adsorption at 300 K.

The high-temperature behaviour of the 13.5 eV loss is in harmony with the characteristics of the desorption of CO. Its intensity decreased when (according to the TDS measurements) the desorption of CO set in, and it disappeared when the desoprtion of CO was complete.

In conclusion, we can state that the isocyanate species is very unstable on the Pt(110) surface and dissociates entirely to adsorbed nitrogen and carbon monoxide at 310–330 K.

The high instability of the NCO species on Pt has recently been confirmed by infrared spectroscopic measurements [31]. Platinum was dispersed on a NaCl window and placed in the vacuum infrared cell described previously [3]. In this case we were able to investigate the infrared spectrum of the NCO species on the Pt itself, without the disturbing effect of the oxidic support. The adsorption of HNCO on this surface at 150 K produced a relatively strong absorption band at 2180 cm^{-1}, which belongs to NCO species bonded to Pt. (Molecularly bonded HNCO gives a band at 2260 cm^{-1}.) The NCO band in this case appeared at much lower frequencies than on supported Pt, and it was much more unstable [1,3,7–11]. On elevation of the temperature, a decrease in the intensity of this band was observed; the band disappeared entirely at 330 K.

Recent *high resolution* electron energy loss spectroscopic measurements on a Pt(111) surface also indicated the instability of the NCO species on Pt [32]. In this

case the NCO band, indicative of the dissociation of HNCO, appeared at 150 K and disappeared above 250 K.

Taking into account the above conclusion, as well as the observation that the adsorption of atomic nitrogen on this surface produced a (2 × 2) LEED pattern at a low coverage [29], the (2 × 2) surface structure found after HNCO adsorption at 300 K is very probably due to the adsorbed nitrogen formed in the dissociation of the NCO species. It appears that the adsorbed CO also formed in the dissociation of NCO does not influence the formation of this ordered structure of adsorbed nitrogen. This was confirmed by a separate study [29]. In contrast to the adsorptions of CO [23,24] and atomic N [29], the adsorption of HNCO at 300 K and its dissociation products did not result in the reordering of the surface Pt atoms from the (1 × 2) to the (1 × 1) arrangement. The reason is that the surface concentrations of adsorbed CO and N formed in the dissociation of the NCO species are not high enough to cause this change in the periodicity of the surface Pt atoms.

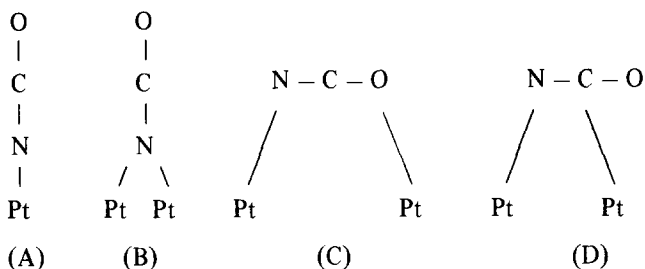## 4.3. Possible bonding modes of HNCO

Let us deal first with the structure of HNCO in the vapour phase. After some earlier controversy, it was shown conclusively by Herzberg [33] that this compound in the vapour phase has the structure H–N=C=O, and should thus properly be called isocyanic acid. Spectroscopic and electron diffraction investigations showed that the NCO group is nearly linear; the H atom is off this straight line at an angle of 125° [33–35]. All four atoms are most probably in one plane and the N–C and C–O distances are almost equal (table 3).

Any model suggested for the bonding of the NCO species to Pt should account for the relatively easy fission of the N–C bond in the NCO species on this surface. Assumption of a terminal coordination via the nitrogen atom (A) does not seem

Table 3
Some structural parameters for HNCO

		Spectroscopic studies [35], distances (Å)	Electron diffraction studies [34], distances (Å)
H–N–C	angle	128°5' ± 30'	125° (estimated)
C–O	distance	1.171 ± 0.01	1.19 ± 0.03
N–C	distance	1.207 ± 0.01	1.19 ± 0.03
N–H	distance	0.987 ± 0.01	1.01 (estimated)
N–O	distance	2.378 ± 0.005	2.38 ± 0.03

to explain this feature, and the same is valid for the simple bridge structure (B):

```
O         O
|         |
C         C        N — C — O        N — C — O
|         |        /       \        /       \
N         N       /         \      /         \
|        / \     /           \    /           \
Pt    Pt   Pt   Pt           Pt  Pt           Pt
(A)     (B)          (C)                 (D)
```

It would be more appropriate to assume that the *NCO is multiply bonded to the surface*. We may presume that the NCO group lies more or less parallel to the surface Pt atoms and is bonded via both the nitrogen and oxygen atoms (C). This bridge structure was proposed for the isocyanate complexes of transition metals on the basis of their magnetic and spectral properties [36].

An alternative form could be that the NCO is bonded to the Pt via nitrogen and carbon atoms (D), similarly as in the case of CN groups [27,28,37,38].

Although the present measurements do not permit deductions regarding the structure of the NCO species on Pt, it is conceivable that the dissociation of the N–C bond proceeds more easily in the latter structural forms (C and D).

Taking into account the arrangement of the surface Pt atoms in the clean (1 × 2) structure, we propose that, in analogy with the adsorption of oxygen [16], the NCO is located in the "troughs" of the corrugated surface, so that the plane of the NCO is parallel with that of the (111) microfacets (fig. 11). At these sites there is a high probability of the multiple bonding of NCO with surrounding Pt atoms, and hence for its dissociation.

It is instructive at this stage to compare the stability of the NCO group with that of CN on the same Pt surfaces, and also with the stability of the NCO group on a
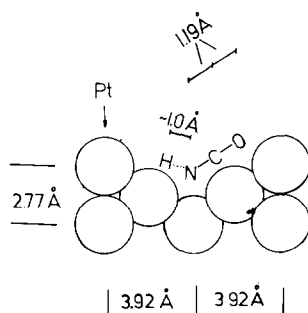
Fig. 11. Proposed model for the arrangement of NCO in the missing row model of the Pt(110) (2 × 1) surface.

Cu surface. It appears that although the CN group is also strongly bonded to Pt, no rupture of the C—N bond occurs, and the CN recombines and desorbs as C_2N_2 above 673 K [27,28]. This is in harmony with the expectation that the C—N bond in NCO is much weaker than the triple bond in the CN group. (The cleavage of this bond in the CN group does occur on the Ni(111) face, however, as indicated by the complete removal of nitrogen as N_2 at 800 K [38].)

The NCO group was found to be much more stable on a Cu(111) surface than on the Pt surface [12]. A possible reason is that, in sharp contrast to Pt, the Cu—C bond strength is very low (no bonding of CO occurs on this surface at 300 K), and consequently there is no driving force for the rupture of the N—C bond in the NCO species on Cu surfaces.

References

[1] M.L. Unland, J. Catalysis 31 (1973) 459.
[2] J.W. London and A.T. Bell, J. Catalysis 31 (1973) 96.
[3] F. Solymosi, J. Sárkány and A. Schauer, J. Catalysis 46 (1977) 297.
[4] M.F. Brown and R.D. Gonzalez, J. Catalysis 44 (1976) 477.
[5] F. Solymosi and J. Sárkány, Appl. Surface Sci. 3 (1979) 68.
[6] B.A. Morrow, W.N. Sont and A.St. Onge, J. Catalysis 62 (1980) 304.
[7] H. Niiyama, M. Tanaka, H. Iida and E. Echigoya, Bull. Chem. Soc. Japan 49 (1976) 2047.
[8] D'Arcy Lorimer and A.T. Bell, J. Catalysis 59 (1979) 223.
[9] F. Solymosi, J. Kiss and J. Sárkány, in: Proc. 7th Intern. Vacuum Congr. and 3rd Intern. Conf. on Solid Surfaces, Vienna, 1977, Eds. R. Dobrozemsky et al. (Vienna, 1977) p. 819.
[10] F. Solymosi, L. Völgyesi and J. Sárkány, J. Catalysis 54 (1978) 336.
[11] F. Solymosi, L. Völgyesi and J. Raskó, Z. Physik. Chem. (NF) 120 (1980) 79.
[12] F. Solymosi and J. Kiss, in: Proc. IVC-8, ICSS-4, ECOSS-3, Cannes, 1980, p. 213; F. Solymosi and J. Kiss, Surface Sci. 104 (1981) 181.
[13] F. Solymosi and T. Bánsági, J. Phys. Chem. 83 (1979) 552.
[14] K. Schwaha, PhD Thesis, Innsbruck (1976).
[15] J.L. Gland, Surface Sci. 71 (1978) 327.
[16] R. Ducros and R.P. Merrill, Surface Sci. 55 (1976) 227.
[17] M. Wilf and P.T. Dawson, Surface Sci. 65 (1977) 359.
[18] F.P. Netzer and J.A.D. Matthew, Surface Sci. 51 (1975) 352, and references therein.
[19] F.P. Netzer, R.A. Wille and J.A.D. Matthew, Solid State Commun. 21 (1977) 97.
[20] A. Seignac and S. Robin, Solid State Commun. 11 (1972) 217.
[21] M. Fink, M.R. Martin and G.A. Somorjai, Surface Sci. 29 (1972) 303.
[22] J.A.D. Matthew, R.A. Wille and F.P. Netzer, Surface Sci. 67 (1977) 269.
[23] H.P. Bonzel and R. Ku, Surface Sci. 33 (1972) 91.
[24] C.M. Comrie and R.M. Lambert, Faraday Trans. II, 72 (1976) 1659.
[25] C.M. Comrie, W.H. Weinberg and R.H. Lambert, Surface Sci. 57 (1976) 619.
[26] P.D. Reed and R.M. Lambert, Surface Sci. 57 (1976) 485.
[27] M.E. Bridge and R.M. Lambert, Surface Sci. 63 (1977) 315.
[28] M.E. Bridge and R.M. Lambert, Surface Sci. 57 (1976) 415.
[29] J. Kiss, A. Berkó and F. Solymosi, in: Proc. IVC-8, ICSS-4, ECOSS-3, Cannes, 1980, p. 521.
[30] R.W. McCabe and L.D. Schmidt, Surface Sci. 60 (1976) 85.

[31] F. Solymosi and J. Raskó, J. Catalysts, in press.
[32] B.A. Sexton, private communication.
[33] G. Herzberg and C. Reid, Disc. Faraday Soc. 9 (1950) 92.
[34] E.H. Eyster, R.H. Gillette and L.V. Brockway, J. Am. Chem. Soc. 62 (1940) 3226.
[35] J.H. Jones, J.N. Shoolery, R.G. Shulman and D.M. Yost, J. Chem. Phys. 18 (1950) 990.
[36] H.C.A. King, E. Körös and S. Nelson, Nature 196 (1962) 572; J. Chem. Soc. (1963) 5449; (1964) 4832.
[37] F.P Netzer, Surface Sci. 61 (1976) 343.
[38] J.C. Hemminger, E.L. Muetterties and G.A. Somorjai, J. Am. Chem. Soc. 101 (1979) 62.